Title: Executive and Attentional Information Transfer Hubs of the Human Causal Connectome

Authors: Eric Rawls[1]*, Erich Kummerfeld[2], Bryon A. Mueller[1], Sisi Ma[2], and Anna Zilverstand[1,3]

Affiliations: [1]Department of Psychiatry and Behavioral Sciences, University of Minnesota, [2] Institute for Health Informatics, University of Minnesota, [3]Medical Discovery Team on Addiction

*Correspondence: Eric Rawls, rawls017@umn.edu

Abstract

We introduce a data-driven causal discovery method (Greedy Adjacencies and Non-Gaussian Orientations; GANGO) for calculating a "causal connectome" of directed connectivity from resting-state fMRI data. Prominent directed information transfer hubs of the causal connectome were situated in attentional (dorsal attention) and executive (frontoparietal and cingulo-opercular) networks. These hub networks had distinctly different connectivity profiles. Attentional networks shared incoming connections with sensory regions and outgoing connections with higher cognitive networks, while executive networks primarily connected to other higher cognitive networks and had a high degree of bidirected connectivity. Virtual lesion analyses accentuated these findings, demonstrating that attentional and executive hubs are points of critical vulnerability in the human causal connectome. These data highlight the central role of attention and executive control networks in the human cortical connectome and set the stage for future applications of data-driven causal ("effective") connectivity analysis in psychiatry.

Keywords: effective connectivity, causal discovery, connectome, resting-state, hubs, centrality, frontoparietal, biomarker, causal modeling

1 Introduction

Brain network interactions give rise to the neural capacity for information processing and cognition (Bressler, 1995; E. Bullmore & Sporns, 2009; Friston, 2002; McIntosh, 2000). These networks have a non-random topological organization (Bullmore & Sporns, 2009), including the presence of both segregated modules (Meunier et al., 2009, 2010) and a small number of highly connected nodes (Achard et al., 2006; Eguiluz et al., 2005; Sporns et al., 2007; van den Heuvel & Sporns, 2013), the "hubs" of the connectome (Sporns et al., 2007; van den Heuvel & Sporns, 2013). These hubs coordinate the transfer of large amounts of information through brain circuits and play a critical role in coordinating neural responses that enable flexible behavior. In the 302-neuron connectome of *C. Elegans* (Varshney et al., 2011; White et al., 1986), both segregated modules (Pavlovic et al., 2014; Sohn et al., 2011) and highly connected hubs (Arnatkevičiūtė et al., 2018) were confirmed. Using data from 461 tract-tracing experiments to reconstruct the mouse cortical connectome, Rubinov and colleagues (2015) also confirmed the presence of highly connected hubs that were optimally situated to coordinate information transfer between segregated brain modules. Concerted efforts are underway to examine the human connectome in the same way (Sporns, 2012, 2013; Sporns et al., 2005; Van Essen et al., 2013; Van Essen & Ugurbil, 2012). Here we present data on a "causal connectome" derived from resting-state neuroimaging data using a data-driven causal discovery method that can estimate directed connections, to characterize the effective connectivity of the resting-state functional connectome.

To investigate information transfer in this "causal connectome", we looked at the interaction between brain networks and their function as information transfer "hubs". Network hubs are typically examined using centrality, a set of metrics that quantify the capacity of a node in a graph to influence (or be influenced by) other nodes. Over 100 measures of centrality have been proposed (Jalili et al., 2015), only a subset of which are commonly applied to brain network analysis (Rubinov & Sporns, 2010; van den Heuvel & Sporns, 2013). The most common is degree centrality (the number of connections attached to each node), which has a simple and intuitive interpretation, but alone provides limited information. For example, a node might have relatively few connections, but still act as an important bottleneck for

communication between many other nodes in the network. Thus, other centrality measures can be used to capture a more nuanced view of brain network hubs, the most prototypical of which is betweenness centrality (how often a node lies on the shortest path between two other nodes). Different metrics for centrality are often highly correlated with each other (Oldham et al., 2019; Oldham & Fornito, 2019), but some centrality metrics may be more appropriate for certain types of networks than for others. For example, while degree centrality is frequently used for characterizing structural brain hubs (Crossley et al., 2014; Rubinov et al., 2015), degree in correlation-based fMRI networks is biased to identify nodes that primarily connect within a local sub-network of the brain (Power et al., 2013; van den Heuvel & Sporns, 2013). Thus, early degree-based analyses often identified high-degree nodes in the default mode network (Buckner et al., 2009; Cole et al., 2010; Power et al., 2013; Tomasi & Volkow, 2011; van den Heuvel & Sporns, 2013), one of the brain's largest resting-state subnetworks. Because of this confound, fMRI Pearson correlation-based network analyses has considered alternative methods for identifying functional hubs, including metrics that consider the diversity of between-subnetwork connections of a node such as participation coefficient (Bertolero et al., 2018; Grayson et al., 2014; Power et al., 2013; Reber et al., 2021), and coactivation/connectivity over multiple cognitive tasks (Cocuzza et al., 2020; Cole et al., 2013; Crossley et al., 2013, 2014; Ray et al., 2020). These more recent analyses, based on the capacity of brain nodes to link and interact with a diverse variety of other brain networks, instead reveal a set of brain hubs distributed broadly through frontal, parietal, and temporal cortices.

However, fMRI connectivity methods have typically been limited to undirected connectivity, providing information about connected brain regions (hereafter adjacencies), but not the direction of these connections (hereafter orientations). The need to extend studies of human brain connectivity to directed (effective) connectivity measures is recognized (Ramsey et al., 2010; Reid et al., 2019; Smith, 2012; Valdes-Sosa et al., 2011), but methods for fMRI effective connectivity are limited (Ramsey et al., 2010, 2014; Sanchez-Romero et al., 2019; Smith et al., 2011). Granger prediction (Granger, 1969) attempts to recover causal influences using time-lagged regressions but has negligible accuracy in detecting adjacencies or orientations in simulated fMRI data (Smith et al., 2011). GIMME (Gates & Molenaar,

2012), a group-level algorithm that also uses time lags to infer causality, achieves better performance, but is computationally intensive and can only scale to a small number of brain regions (Sanchez-Romero et al., 2019). Dynamic causal modeling (DCM) builds a generative model of the neural basis of the fMRI signal (Friston et al., 2003), but is designed for use in a task-based context and is generally not scalable enough to support whole-cortex analyses (but see recent advances in regression-DCM [Frässle et al., 2021]). However, methods grounded in causal discovery show high promise for uncovering causal connectivity from fMRI (Mumford & Ramsey, 2014; Ramsey et al., 2014; Sanchez-Romero et al., 2019), and for dealing with the high dimensionality of whole-cortex data (Ramsey et al., 2017). Suitable combinations of causal discovery-based methods can achieve near-perfect (>90%) accuracy in simulated fMRI data (Hyvärinen & Smith, 2013; Ramsey et al., 2014), and can even achieve high accuracy in uncovering feedback cycles (Sanchez-Romero et al., 2019).

In the current study, we capitalize on these recent advances in causal discovery machine learning to build whole-cortex effective connectomes from single-subject resting-state fMRI data, introducing a two-step causal discovery framework called GANGO (Greedy Adjacencies and Non-Gaussian Orientations). We first estimate whole-cortex adjacencies using Fast Greedy Equivalence Search (Chickering, 2002; Ramsey et al., 2017; Ramsey, 2015), resulting in a sparse graph without the false positive connections produced by both full and partial correlation approaches (Reid et al., 2019). This method has high accuracy for adjacencies, but low accuracy for orientations (Smith et al., 2011). Thus, we follow this initial adjacency search with a pairwise edge orientation algorithm that exploits non-Gaussian information in the BOLD signal (Hyvärinen & Smith, 2013), shown in (Ramsey et al., 2014; Sanchez-Romero et al., 2019) to have excellent performance (>90% accuracy) in determining edge orientation of the Smith and colleagues (2011) simulations. We thus obtain, on a single-subject basis, a whole-cortex graph summarizing dominant directed information flow patterns between regions. We focus investigation on the hub structure of this novel directed or “causal” connectome, demonstrating critical hub roles and distinct causal connectivity profiles of the dorsal attention network, frontoparietal network, and cingulo-opercular network.

2 Results

2.1 Whole-Cortex Effective Connectivity Graphs are Sparse but Well-Connected

We studied "causal" or effective network connectivity properties of the human cortex using a large sample (n = 442) of high-quality resting-state fMRI data (Glasser et al., 2013; Marcus et al., 2013; Smith et al., 2013; Uğurbil et al., 2013; Van Essen et al., 2013). Each subject's resting-state data was collected over two days in two sessions with 2 runs per session (14:33/1200 volumes per run). We analyzed only one day of data (two runs, 2400 volumes; z-scored and concatenated) to limit potential state influences on fMRI measures. We parcellated each subject's cortex into 360 regions using a recently developed multimodal parcellation (Glasser et al., 2016) and estimated sparse cortical effective connectivity graphs on a per-subject basis using a two-step method proposed in (Ramsey et al., 2014). We first estimated a set of adjacencies (directly connected regions) using a greedy search over the entire set of possible directed acyclic brain graphs (Ramsey et al., 2017; Ramsey, 2015), then estimated the causal direction of each edge using outlier-robust skew-based pairwise likelihood ratios (Hyvärinen & Smith, 2013). The resulting effective connectivity networks were sparse, containing only ~2.25% of all possible connections (360 parcels: mean n connections = 1452). Nevertheless, the graphs were well-connected – in most graphs (93.7%), every node was connected to at least one other node, and of the 6.3% of graphs that contained disconnected nodes, each graph had very few disconnected nodes (median = 1, max = 2). Thus, despite the sparsity of the cortical effective connectivity graphs we analyzed, these graphs appear to adequately capture global causal patterns of connectivity.

2.2 Diversity of Inter-Network Connections Highlights Hub Roles of Multiple Brain Networks

To summarize the overall connectivity structure of our cortical effective connectivity graphs, we categorized each of 360 cortical nodes into 12 resting-state networks (RSNs; Ji et al., 2019). We first examined patterns of connectivity between these large-scale brain RSNs. We established whether each RSN shared a statistically significant proportion of connections with each other RSN. To do this, we first calculated the number of edges shared by each pair of RSNs for each subject. Then, across subjects and for each pair of RSNs, we determined whether the proportion of shared edges exceeded that expected

under the null hypothesis of chance-level connectivity using Wilcoxon rank-sum tests against an empirical null hypothesis of random inter-RSN connectivity. We additionally tested for a preferred direction of connectivity between significantly connected pairs of RSNs. For each subject and for each pair of significantly connected RSNs, we computed the number of connections separately for incoming and outgoing connections. That is, for significantly connected RSNs A and B, we separately calculated the number of edges that went from A to B, and the number of edges from B to A. Across subjects, we then determined whether these numbers of connections differed, signifying a preferred direction of connectivity between RSNs.

These analyses enabled us to generate a consensus diagram of how the 12 RSNs are interconnected (*Figure 1a*). A clear hub-periphery structure was apparent when the consensus connectivity plot was shown using a force-directed layout (*Figure 1a*). We found that visual RSNs 1 and 2 were tightly bidirectionally interconnected, and that visual RSNs projected to the dorsal attention network. The dorsal attention network projected to multimodal association networks (posterior and ventral) and the frontoparietal network. The frontoparietal network was situated in the center of the graph, being the most highly connected RSN and sending information to the ventral attention/language, limbic/orbito-affective, and default mode RSNs, while bidirectionally sharing connections with the cingulo-opercular network.

We supplemented this analysis by an examination of the average participation coefficient within each RSN. We calculated participation coefficient for each node (n = 360) in each subject's graph, and for each subject participation coefficient values were averaged within each of 12 RSNs. Since we used causal/effective connectivity graphs, we calculated participation coefficient separately using outgoing and incoming connections, resulting in two summary measures per RSN, per subject (hereafter out-part and in-part, respectively). We found that across subjects, the twelve RSNs differed substantially in both out-part and in-part (Kruskall-Wallis tests; both $p < .001$). Post hoc comparisons (Tukey HSD) demonstrated similar patterns of RSN differences for out-part and in-part. The posterior multimodal and dorsal attention RSNs demonstrated the highest participation coefficient values, followed by the frontoparietal, ventral

attention, cingulo-opercular, and visual-1 RSNs (all $p < .001$). This analysis of participation coefficients demonstrated that the dorsal attention, posterior multimodal association, frontoparietal, ventral attention, cingulo-opercular, and visual-1 RSNs maintain the greatest diversity of inter-RSN connections in the effective cortical connectome (*Figure 1bc*).

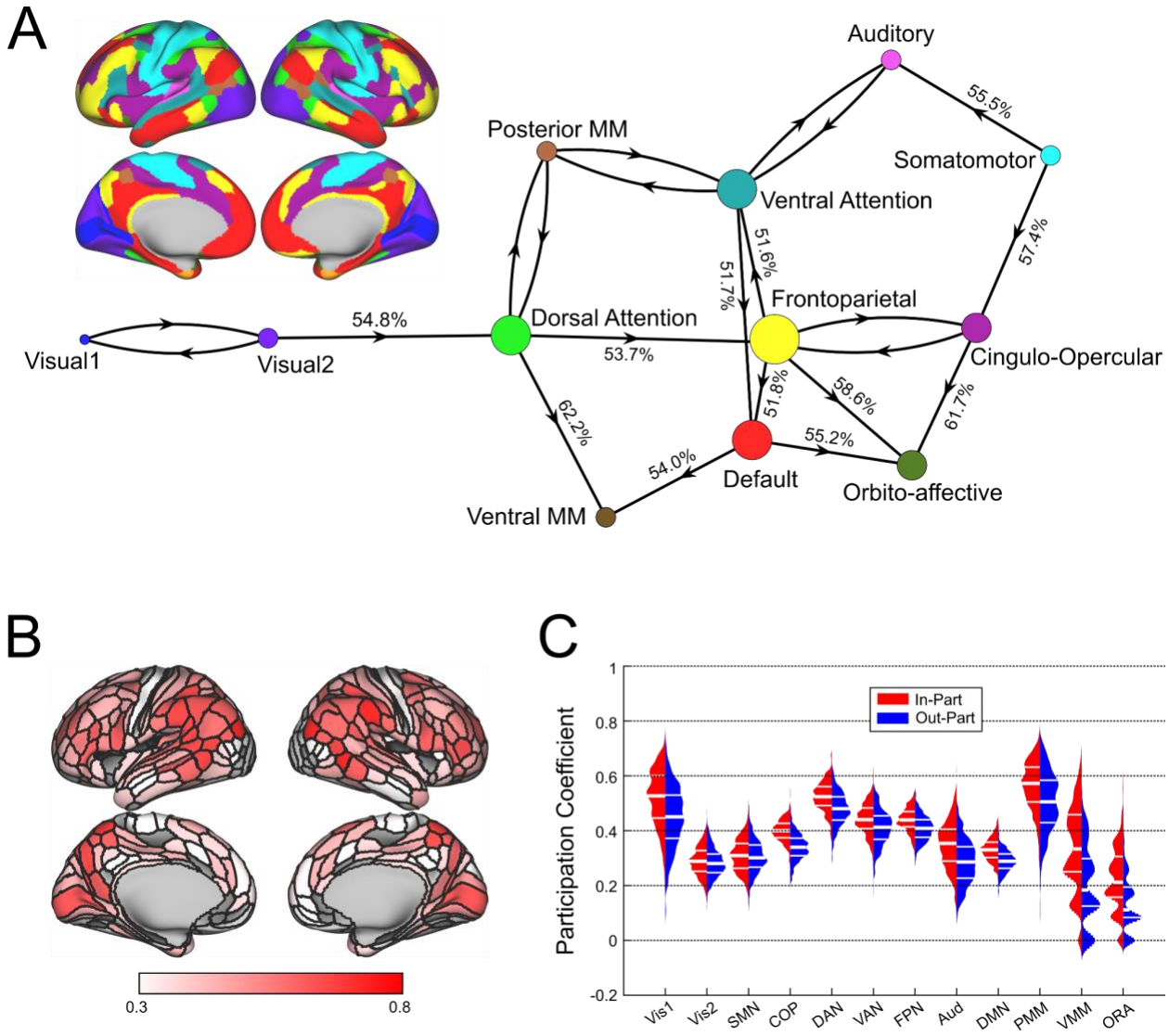

Figure 1. Diversity of Inter-Network Connections Highlights Hub Roles of Multiple Brain Networks. A: Significant inter-RSN connectivity of the cortical effective connectivity network, plotted in a force-directed layout. A clear hub-periphery structure emerged. The dorsal attention network formed a causal

pathway from early visual RSNs to multimodal association RSNs. The frontoparietal network was situated in the center of the graph and overall the most interconnected RSN, receiving effective connections from dorsal attention network, sending effective connections to ventral attention/language, limbic/orbito-affective, and default mode networks, and sharing bidirectional connections with cingulo-opercular network. Percentages on directed connections indicate the proportion of shared connections that were oriented in the statistically preferred direction.

B: Nodal in-connection and out-connection participation coefficient values plotted on an average inflated cortical surface. Prominent high-participation nodes were apparent in parietal and frontal cortex.

C: RSN average participation coefficients. Generally, the posterior multimodal, dorsal attention, frontoparietal, ventral attention, cingulo-opercular, and visual-1 RSNs maintained a high diversity of out-of-RSN connections compared to the rest of the cortex.

2.3 The Effective Cortical Connectome Has a Heavy-Tailed Centrality Structure

Thus far we have clarified patterns of inter-RSN connectivity in the cortical effective connectome. From here, we examined the most important hubs of the cortical effective connectome using two common centrality metrics: degree centrality, which characterizes highly connected nodes, and betweenness centrality, which characterizes nodes that lie on many shortest paths between other nodes and thus facilitate efficient network communication (Rubinov & Sporns, 2010). If nodes are to be considered hubs based on centrality metrics, the distribution of those metrics should be heavy tailed, with a minority of highly central nodes. We found that the centrality distributions of the obtained causal graphs were indeed heavy-tailed, with most nodes having very low centrality and relatively few nodes having very high causal centrality (*Figure 2a,b,c,d*). Centrality values of the effective connectivity graphs were significantly more heavy-tailed than equally connected random comparison graphs, as confirmed by comparing the skewness of the indegree, outdegree, total degree, and betweenness distributions of these two sets of graphs (rank-sum tests, all $p < .001$).

2.4 The Most Central Hubs of the Causal Connectome Cluster in Executive and Attentional Networks

For each subject-level effective connectivity graph, we calculated the indegree, outdegree, total degree, and betweenness centrality of each of 360 nodes, and averaged these nodal metrics within each of 12 RSNs. Across subjects, we then tested whether these 12 RSNs differed in average centrality metrics. The 12 RSNs differed in average indegree, outdegree, and total degree (Kruskal-Wallis tests, all $p < .001$). Most relevant for the current work, post hoc testing for RSN degree differences (Tukey's honest significant difference) demonstrated that the dorsal attention and frontoparietal networks had significantly higher indegrees, outdegrees, and total degrees than the other 10 RSNs (all $p < .001$). Similarly, comparison of average betweenness centrality across the 12 RSNs (*Figure 2j*) established that frontoparietal nodes participated in the greatest number of efficient paths, followed by dorsal attention nodes; these RSNs had higher betweenness centrality averages than the other 10 RSNs, and frontoparietal had significantly higher betweenness than dorsal attention (all $p < .001$). The cingulo-opercular network had the third highest average betweenness centrality scores, despite having only modest degree centrality, thus suggesting that while cingulo-opercular regions might not be the most highly connected regions in cortex, these regions are nevertheless particularly important for cortical communication. Note that while (Power et al., 2013) showed that degree-based hubs in Pearson correlation networks are confounded by the size of the functional communities the nodes belong to (i.e, the number of nodes in each RSN), in a critical control analysis we did not find significant correlations between community size and degree or betweenness centrality (*Figure 2k,l,m,n)*, suggesting that our measures of effective connectivity hubs based on centrality cannot be ascribed to the size of the RSNs in our analysis.

2.4 Executive and Attentional Networks Equally Send and Receive Connections

Since effective connectivity graphs separate incoming and outgoing causal connections, we were additionally able to assess whether each RSN primarily sent or received information. For each subject-level graph, we separately calculated nodal indegree and outdegree, then averaged these values within each of 12 RSNs. We categorized each RSN as primarily receiving or primarily sending connections

using Wilcoxon signed-rank tests of RSN indegree vs. outdegree (corrected for n = 12 multiple comparisons using false discovery rate [FDR]). Most RSNs could be characterized as either primarily "senders" (visual, somatomotor), or as primarily "receivers" (cingulo-opercular, auditory, default mode, posterior/ventral multimodal, and limbic/orbitoaffective). However, a small number of RSNs were found to send and receive equal numbers of connections (frontoparietal, dorsal attention, ventral attention/language; *Figure 2i*).

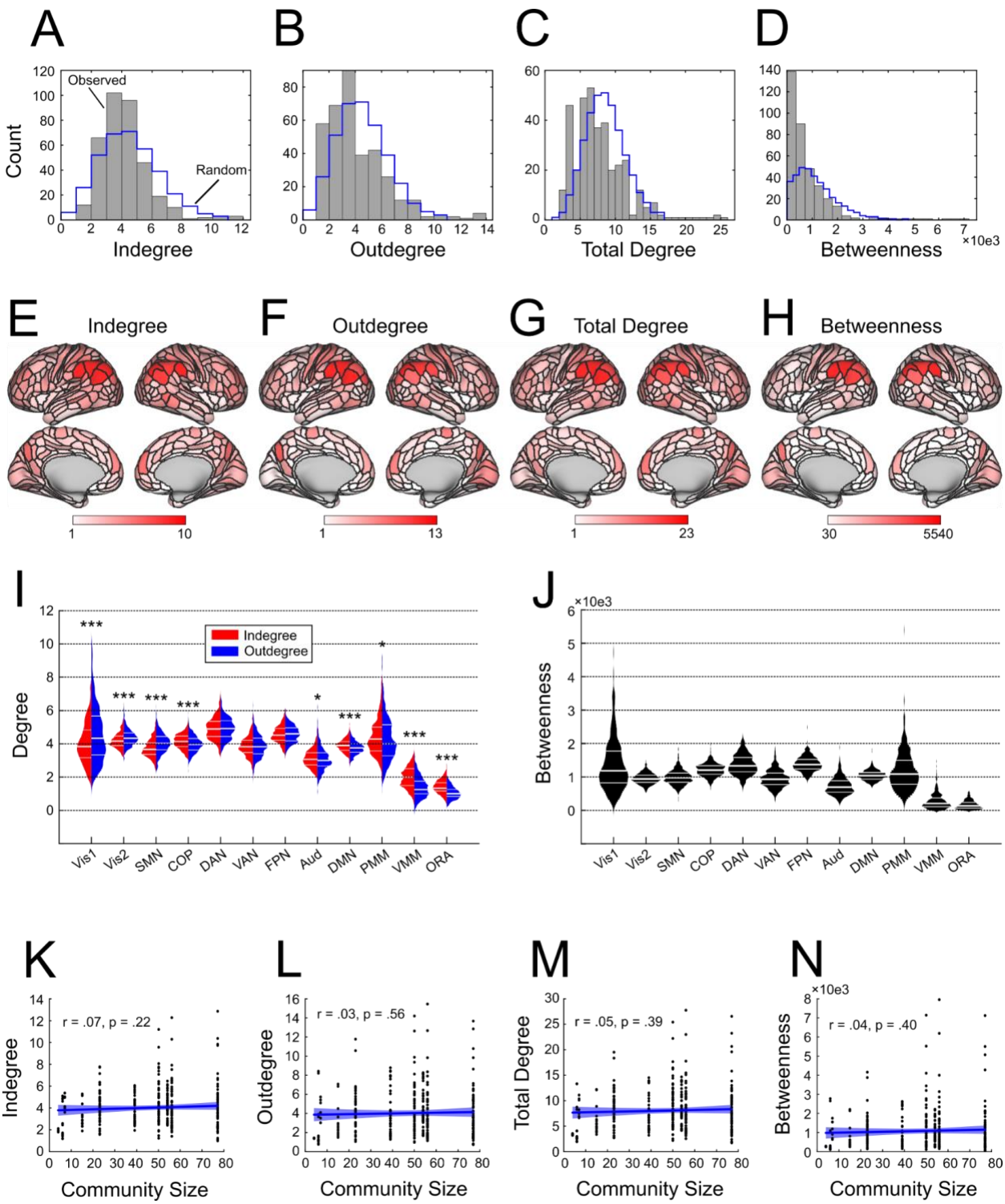

Figure 2. The Most Central Hubs of the Causal Connectome Cluster in Executive and Attentional Networks.

A,B,C,D*: Median nodal centrality across n = 442 subjects, for each of 360 cortical nodes. Blue histogram indicates the distribution of median centralities for 1000 equally connected random graphs.*

E,F,G,H*: Centrality values plotted on inflated cortical surfaces to visualize the anatomical locations of highly connected hubs.*

I: *Average indegree and outdegree across the 12 RSNs. Visual (Vis1 and Vis2) and somatomotor (SMN) networks could be categorized as primarily sending information; cingulo-opercular (COP), auditory (Aud), default mode (DMN), posterior and ventral multimodal (PMM and VMM), and orbitoaffective/limbic (ORA) networks could be classified as primarily receiving information, and dorsal attention (DAN), ventral attention/language (VAN), and frontoparietal (FPN) networks equally sent and received information. Overall, the most connected RSNs were the dorsal attention and frontoparietal networks. * $p < .05$, ** $p < .01$, *** $p < .001$.*

J: *Average betweenness across the 12 RSNs. Overall, frontoparietal network participated in the highest number of short paths, followed by dorsal attention and cingulo-opercular networks.*

K,L,M,N: *Control analyses ruled out the possibility that cortical hubs could be explained by the number of parcels in the RSN that each node belongs to. Blue line indicates a least-squares regression fit, and blue shading indicates the 95% confidence interval of the regression.*

2.5 Executive and Attentional Hubs are Points of Effective Network Vulnerability

Our analyses up to this point have demonstrated that the frontoparietal, dorsal attention, and cingulo-opercular RSNs are critical hubs for facilitating connectome-wide information transfer. It is likely that the identified hubs of the cortical effective connectome are also points of system-level vulnerability to insult. To test this hypothesis, we conducted a series of simulated attacks on the cortical effective connectivity network. In a typical virtual lesion analysis, nodes are deleted sequentially, and the overall impact of node deletion on the brain network is recorded via loss of global efficiency (the average inverse shortest distance between nodes). Generally, this analysis proceeds by deleting high-degree hubs, and recording the loss-of-efficiency (compared to the loss-of-efficiency when random nodes are deleted). We

modified this procedure, to instead examine the impact of specific RSN lesions on the overall network efficiency. For each of the 12 RSNs, we sequentially deleted nodes in that RSN from each subject's cortical graph, and measured loss-of-function via percent change in global efficiency (Latora & Marchiori, 2001; Rubinov & Sporns, 2010), compared to baseline (*Figure 3a*). We fit a linear regression to the global efficiency loss curve for each subject and RSN (plus random deletion, as a control analysis; *Figure 3b*). We then compared the slope of this linear regression across RSNs to see which RSN resulted in the steepest (most rapid) loss of function when lesioned. We additionally recorded network loss-of-function as each of 360 single nodes were deleted, to view the most important anatomical nodes on the cortical surface (*Figure 3d*). Results indicated that the RSN loss functions differed significantly in slope (Kruskal-Wallis $p < .001$). Post-hoc multiple testing (Tukey HSD) indicated that the frontoparietal network had the steepest loss-of-efficiency function, followed by the dorsal attention network. These RSNs had steeper loss functions than the other 10 RSNs (all $p < .001$). Visual-1, cingulo-opercular, and posterior multimodal network also showed strong efficiency loss effects when lesioned. In summary, the targeted attack analysis demonstrated that the hub RSNs we previously identified (frontoparietal, dorsal attention, cingulo-opercular) are critical points of vulnerability in cortical efficiency, and that loss-of-function (virtual lesions) in these RSNs impairs global cortical information transfer to a greater degree than other RSNs.

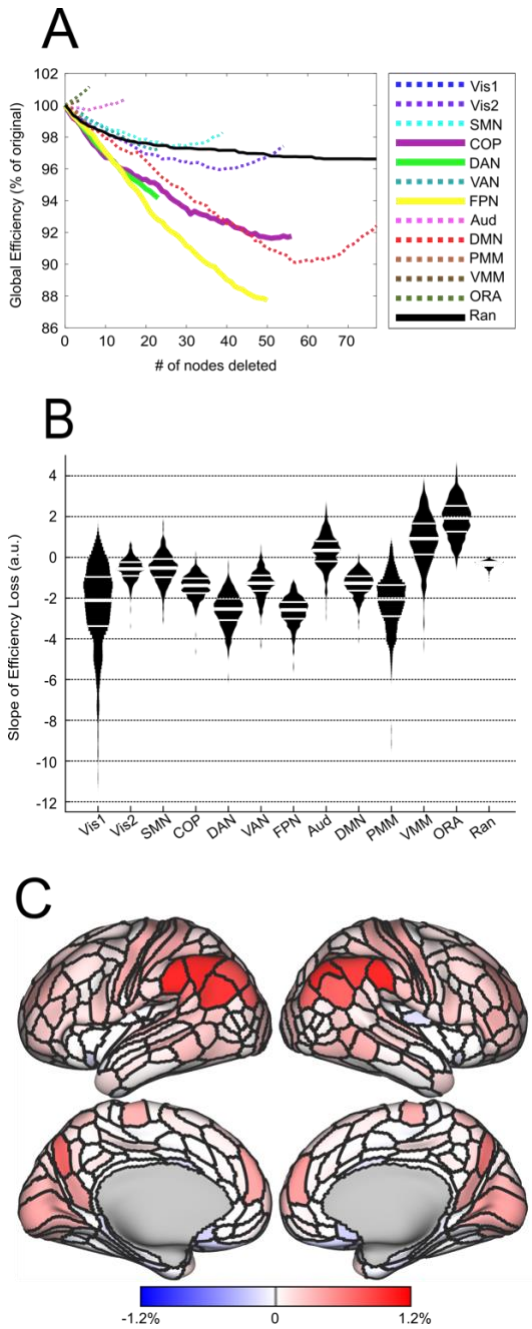

*Figure 3. Executive and Attentional Hubs are Points of Effective Network Vulnerability***.**

A: *Loss of network efficiency following node deletion as a percentage of network global efficiency. The resulting efficiency loss lines are color-coded by RSN. Previously identified hub RSNs (cingulo-opercular, frontoparietal, dorsal attention) are plotted with solid lines, and non-hub RSNs are plotted with dotted lines. Additionally, a random attack was carried out (black line) by deleting nodes chosen at random (rather than from a specific RSN).*

B: *We calculated the slope of the loss line (via linear regression) for each RSN, and compared the slopes, thus quantifying how quickly the cortical network loses efficiency when nodes from each RSN are deleted. Violin plots indicate the slope for the efficiency loss function for each RSN (per subject).*

C: *Change in network global efficiency following deletion of individual cortical nodes. Color indicates the loss-of-efficiency when each single node is deleted.*

2.6 Comparison of GANGO Effective Connectivity Graphs with Pearson Correlation Graphs

To examine how the cortical effective connectivity network compare to more typical connectivity analyses (Pearson correlation graphs), we ran all of the presented analyses using binarized correlation graphs, proportionally thresholded at 15% cost (that is, each graph retained the 15% largest positive values) based on the most typical thresholding procedures from the literature (Achard & Bullmore, 2007; Bullmore & Bassett, 2011). Results of these comparison analyses are presented in the Supplement. Overall, this comparison of our primary results with a set of normally thresholded Pearson correlation graphs demonstrate standard centrality measures (degree, betweenness) in Pearson correlation cortical graphs emphasize the importance of sensory regions and motor cortex as cortical hubs, while effective connectivity graphs instead emphasize higher cognitive regions, in particular frontoparietal and cingulo-opercular networks (which did not exhibit hub-like connectivity in any analysis for Pearson correlation graphs). Furthermore, in Pearson correlation graphs we found that both degree and betweenness centrality were highly confounded by the size of the RSN nodes belonged to, unlike in the effective connectivity graphs. These differences between Pearson correlation and effective connectivity graphs were somewhat attenuated when using participation coefficient as a measure. Notably, we observed that applying the virtual lesion analysis to a thresholded Pearson correlation graph resulted in many RSNs increasing global efficiency when deleted. This is likely due to the much greater incidence of completely unconnected nodes in thresholded Pearson correlation graphs, as opposed to the well-connected directed graphs we generated using the GANGO method.

3 Discussion

Functional connectivity analyses of the human cortex typically use undirected connectivity estimates, derived by computing Pearson correlation coefficients between the time series of blood oxygen level-dependent (BOLD) signals of individual brain regions (nodes). The need to extend functional connectivity analyses to causal (effective) connectivity is recognized (Reid et al., 2019; Smith, 2012), but data-driven methods for calculating high-dimensional (*n[nodes]* > 100) effective connectivity graphs within single subjects have not been established yet. Here, we present an examination of the causal/effective information transfer patterns of the human cortex using a combination of machine learning methods for identifying causal models (Greedy Adjacencies and Non-Gaussian Orientations; GANGO). Prominent hubs of the causal connectome overlap many regions previously identified by resting-state fMRI (Achard et al., 2006; Buckner et al., 2009; Tomasi & Volkow, 2011; van den Heuvel & Sporns, 2013; Zuo et al., 2012), with the GANGO method reliably recovering these network properties when applied on a single subject level. Importantly, control analyses indicated that nodal hub metrics (degree, betweenness centrality) were unconfounded by the size of the RSN that nodes belonged to. In contrast, degree and betweenness centrality were strongly confounded by RSN size for thresholded correlation graphs (Supplement). Overall, we found prominent directed information transfer hubs and points of vulnerability of the causal connectome in dorsal attention network (DAN), frontoparietal network (FPN) and cingulo-opercular network (COP), with each of these hub networks showing distinctly different connectivity profiles.

The dorsal attention network (DAN) exhibited theoretically interesting properties that contributed to its high level of connectivity. In our analysis, DAN had among the greatest diversity of connections with other RSNs (measured using participation coefficient), as well as having overall high connectivity (measured using degree centrality) and participating in many efficient paths (measured using betweenness centrality). Our analysis of the inter-RSN connectivity structure of the cortical effective connectome revealed that DAN owed its high centrality to its role in receiving information from visual networks, processing that information, and then transmitting information to multimodal association networks

(posterior/ventral multimodal association networks, FPN). This is in line with long-standing evidence that DAN plays an important role in top-down visual selective attention (Corbetta & Shulman, 2002; Vossel et al., 2014). While we found that causal connections usually progressed from visual to dorsal attention networks, a large proportion of these connections still progressed in the opposite direction as well. Thus, our results support a role of DAN in top-down control over visual systems as well, providing further evidence that the dorsal attention network supports both bottom-up sensory integration and top-down attentional control (Long & Kuhl, 2018).

The cingulo-opercular network (COP) was found to mediate many efficient paths in the cortex (betweenness) and shared a large diversity of inter-RSN connections (participation coefficient) but did not have particularly high connectivity (degree). COP has a role in maintaining task sets, initiating goal-directed behaviors, and consolidating motor programs (Dosenbach et al., 2006, 2008; Fair et al., 2007; Newbold et al., 2021). In our consensus network structure, we found that COP received significant connections from the somatomotor network, sent significant connections to the orbito-affective (reward) network, and was bidirectionally connected to FPN. The uncovered functional connectivity between the reward networks and COP is in line with evidence that COP has a role in coordinating the response of brain reward-related regions (Huckins et al., 2019), and the connectivity between COP and somatomotor networks corroborates evidence that COP plays a role in consolidation, planning, and plasticity of motor regions (Newbold et al., 2021). Connectivity between COP and somatomotor networks also increases through development and is linked to the development of improved cognitive control (Marek et al., 2015). Finally, COP was found to be tightly bidirectionally connected with frontoparietal network, echoing evidence that these RSNs work together as dual cognitive control networks (Dosenbach et al., 2008; Fair et al., 2007; Gratton et al., 2018).

Across all analyses, we found a critical role of frontoparietal executive network (FPN) connectivity. This represents an important point of agreement between our directed network results and recent advances in understanding the role of the FPN in overall function, as well as an important result that we did not find with traditional Pearson correlation graphs (Supplement). Due to its central position,

FPN shared the greatest diversity of inter-RSN connectivity in the consensus graph, including significant received connections from DAN, significant sent connections to the ventral attention, orbito-affective, and default mode networks, and bidirectional connections with COP. This extensive inter-RSN connectivity is in line with previous studies that have used a battery of multiple tasks to demonstrate that FPN flexibly shifts its connectivity patterns to fulfill task demands (Cocuzza et al., 2020; Cole et al., 2013; Crittenden et al., 2016), and is consistent with a theoretical role of FPN as a flexible executive coordinator of overall brain function (Assem et al., 2020; Dosenbach et al., 2006; Duncan, 2010; Fair et al., 2007; Gratton et al., 2018; Marek & Dosenbach, 2018).

This is also consistent with recent control systems perspectives on brain connectivity, which have suggested that FPN has a particular role in shifting brain network configuration into difficult-to-reach cognitive states (Cornblath et al., 2019; Gu et al., 2015; Lee et al., 2020; Tang et al., 2017). The causal connectivity from FPN to default mode network (DMN) deserves particular attention. These RSNs have previously been observed to have opposing interactions on cognition, including attention (Hellyer et al., 2014), working memory (Kelly et al., 2008; Murphy et al., 2020), and cognitive reasoning (Hearne et al., 2015). We found that the connectivity between FPN and DMN preferentially flows from FPN to default mode network, suggesting that FPN might have an executive role in "turning off" or inhibiting the DMN in response to the need for control. The revealed causal hub role of the FPN is among the most important contributions of this study, as typically thresholded Pearson correlation graphs do not show a convincing hub role of FPN (Supplement), despite ample theoretical and experimental evidence that the frontoparietal network is critical for overall organization and control of the connectome.

The current investigation delivers a powerful new framework for quickly computing high-dimensional causal connectivity graphs from observed brain data as well as providing important insight into the hub structure of the causal human connectome, but it is not without limitations. One potential limitation lies in the use of a relatively coarse (n = 12) RSN partition for summarizing cortical hubs (Ji et al., 2019). However, the use of a published RSN partition facilitates interpretation of results, as the results of higher-dimensional (e.g., ICA-based) RSN partitions are often difficult to interpret and require

abstraction via multidimensional statistics to summarize (as in Smith et al., 2015). In the Supplement we report the consensus network structure of these same data using a larger number of RSNs (the 22 neuroanatomical regions reported in the supplement of Glasser et al., 2016). The consensus structure of connectivity between these 22 regions also shows an orderly progression of information from visual sensory regions, to the dorsal and ventral visual streams, through the parietal association cortex, and into the motor and prefrontal cortex. The organization of this more granular effective network also aligns well with recent perspectives on the hierarchical organization of the prefrontal cortex (Badre & Nee, 2018). An additional limitation of these results is that our method for calculating causal connectivity is unable to discover two-cycles (i.e. direct feedback cycles, where A->B and B->A). While two methods have been proposed for fMRI connectivity that are theoretically capable of recovering two-cycles (Sanchez-Romero et al., 2019), these methods have never been used in an applied research context, and often perform worse than the skew-based orientation method we use (Sanchez-Romero et al., 2019). Notably, the GANGO method is capable of discovering 3-cycle or greater feedback loops, so only direct feedback loops remain unmeasured. Nevertheless, as methods for more accurately assessing feedback cycles from fMRI are developed, the framework we propose in the current investigation could be expanded to include such methods.

3.5 Conclusion

Using a causal discovery machine learning framework, we demonstrate that the most important directional hubs of the cortical connectome are situated in the frontoparietal, dorsal attention and cingulo-opercular networks. In particular, the effective cortical connectome highlights high connectivity of the frontoparietal network with all other higher cognitive RSNs. The discovered hub role of the frontoparietal network in the cortical effective connectome is especially attractive, as brain-based therapies for psychiatric conditions typically impact or directly stimulate nodes in the frontoparietal network (Belsher et al., 2021; Ferrarelli & Phillips, 2021; Fitzgerald, 2021; Song et al., 2019; Voigt et al., 2021; Zhang et al., 2021; Zilverstand et al., 2016, 2017). Previously, we even demonstrated that connectivity in the frontoparietal network has downstream causal effects on the severity of alcohol use disorder (Rawls et al.,

2021). As it is applied on a single-subject basis, the GANGO method could potentially even enable individualized causal connectivity-based neuromodulation targeting. Thus, the current study sets the stage for future applications of data-driven effective connectivity applications in psychiatry.

Acknowledgements

Data were provided by the Human Connectome Project, WU-Minn Consortium (Principal Investigators: David Van Essen and Kamil Ugurbil; 1U54MH091657) funded by the 16 NIH Institutes and Centers that support the NIH Blueprint for Neuroscience Research; and by the McDonnell Center for Systems Neuroscience at Washington University. ER is supported by a training grant from the National Institutes of Mental Health (T32-MH115866). The content is solely the responsibility of the authors and does not necessarily represent the official views of the National Institutes of Mental Health.

Author Contributions

ER: Conceptualization, Methodology, Software, Validation, Formal Analysis, Writing – Original Draft, Writing – Review and Editing, Visualization, Funding Acquisition. **EK:** Conceptualization, Methodology, Validation, Writing – Review and Editing, Supervision. **BAM:** Validation, Writing – Review and Editing. **SM:** Validation, Writing – Review and Editing. **AZ:** Conceptualization, Methodology, Validation, Resources, Writing – Review and Editing, Supervision, Project Administration, Funding Acquisition.

Declaration of Interests

The authors confirm that this research was completed in the absence of any financial or non-financial competing interests.

4 Methods

4.1 Subjects

All analyses used publicly available resting-state functional neuroimaging data from 442 unrelated healthy young adult subjects recruited as part of the Washington University – Minnesota (WU-Minn) Human Connectome Project Consortium (56% [n = 248] female; aged 22-35 [mean age = 28.6 years]; https://db.humanconnectome.org/data/projects/HCP_1200) (Barch et al., 2013; Glasser et al., 2013; Marcus et al., 2013; Smith et al., 2013; Uğurbil et al., 2013; Van Essen et al., 2013). All subjects provided written informed consent at Washington University.

4.2 Resting-State fMRI Acquisition and Preprocessing

Structural and functional MRI data were collected at Washington University on a Siemens 3T Connectome Skyra scanner. Full details of the acquisition parameters for the HCP data are described in (Uğurbil et al., 2013). Each subject's resting-state data was collected over two days in four sessions (14:33/session; 1200 samples/session). In this study we analyzed only one day of data (two runs, individually z-scored and concatenated) to limit potential state influences on fMRI measures. Structural and functional data preprocessing is described in (Glasser et al., 2013), and used version 3.21 of the HCP preprocessing pipeline. Structural data preprocessing consisted of bias field and gradient distortion correction, coregistration of T1/T2 images, and registration to MNI space. Cortical surface meshes were constructed using FreeSurfer, transformed to MNI space, registered to individual surfaces, and downsampled. Functional MRI preprocessing consisted of gradient distortion correction, motion correction, EPI distortion correction, followed by T1 registration. Transforms were concatenated and run in a single nonlinear resampling to MNI space followed by intensity normalization. Data were masked by the FreeSurfer brain mask, and volumetric data were mapped to a combined cortical surface vertex and subcortical voxel space ("grayordinates") using a multimodal surface registration algorithm (Robinson et al., 2014) and smoothed with a 2mm FWHM Gaussian in surface space (thus avoiding smoothing over gyral banks). fMRI data were conservatively high-pass filtered with FWHM = 2000 s and cleaned of artifacts using ICA-FIX (Griffanti et al., 2014; Salimi-Khorshidi et al., 2014). Artifact components and 24

motion parameters were regressed out of the functional data in a single step, producing the final ICA-FIX denoised version of the data in CIFTI ("grayordinates") space (Glasser et al., 2016) that was used in subsequent analyses.

4.3 Construction of Whole-Brain Effective Connectivity Graphs

We introduce a computational strategy to define causal connectome graphs on a per-subject basis using a two-step process we refer to as GANGO (Greedy Adjacencies and Non-Gaussian Orientations). Our analysis pipeline began with n = 442 sets of fully preprocessed, multi-modally surface registered, ICA-FIX denoised fMRI data provided by the HCP consortium. We parcellated cortex surface vertices into 360 regions using a recently developed multimodal parcellation (Glasser et al., 2016). In the first step, we defined nodal adjacencies (connected regions) using Fast Greedy Equivalence Search, a greedy score-based causal search algorithm (Ramsey et al., 2017; Ramsey, 2015). This algorithm finds a sparse set of connections between continuous variables by minimizing a penalized likelihood score over the entire graph (Schwarz, 1978). We computed FGES with causal-cmd v1.2.0 (https://bd2kccd.github.io/docs/causal-cmd/) using default parameters (SEM-BIC penalized likelihood score, penalty discount = 1 corresponding to the classic BIC score). FGES has been shown in simulations to obtain highly accurate estimates of nodal adjacencies, but relatively inaccurate orientations (Smith et al., 2011). Therefore, we made the FGES-derived graph undirected by symmetrizing it across the diagonal. We then reoriented the edges using an estimate of the direction of causal effect based on the pairwise likelihood ratio under the linear non-Gaussian acyclic model (Hyvärinen & Smith, 2013). For an intuitive information theoretic perspective on how non-Gaussian information can be used to orient edges between pairs of variables, see (Hyvärinen & Smith, 2013). We used a MATLAB implementation of an outlier-robust skew-based measure of the pairwise likelihood ratio (Hyvärinen & Smith, 2013), which has shown to generate optimal estimates of causal direction in simulated fMRI data (Ramsey et al., 2014; Sanchez-Romero et al., 2019). These steps resulted in n = 442 sparse effective connective graphs, which we characterized using various graph theoretic analyses.

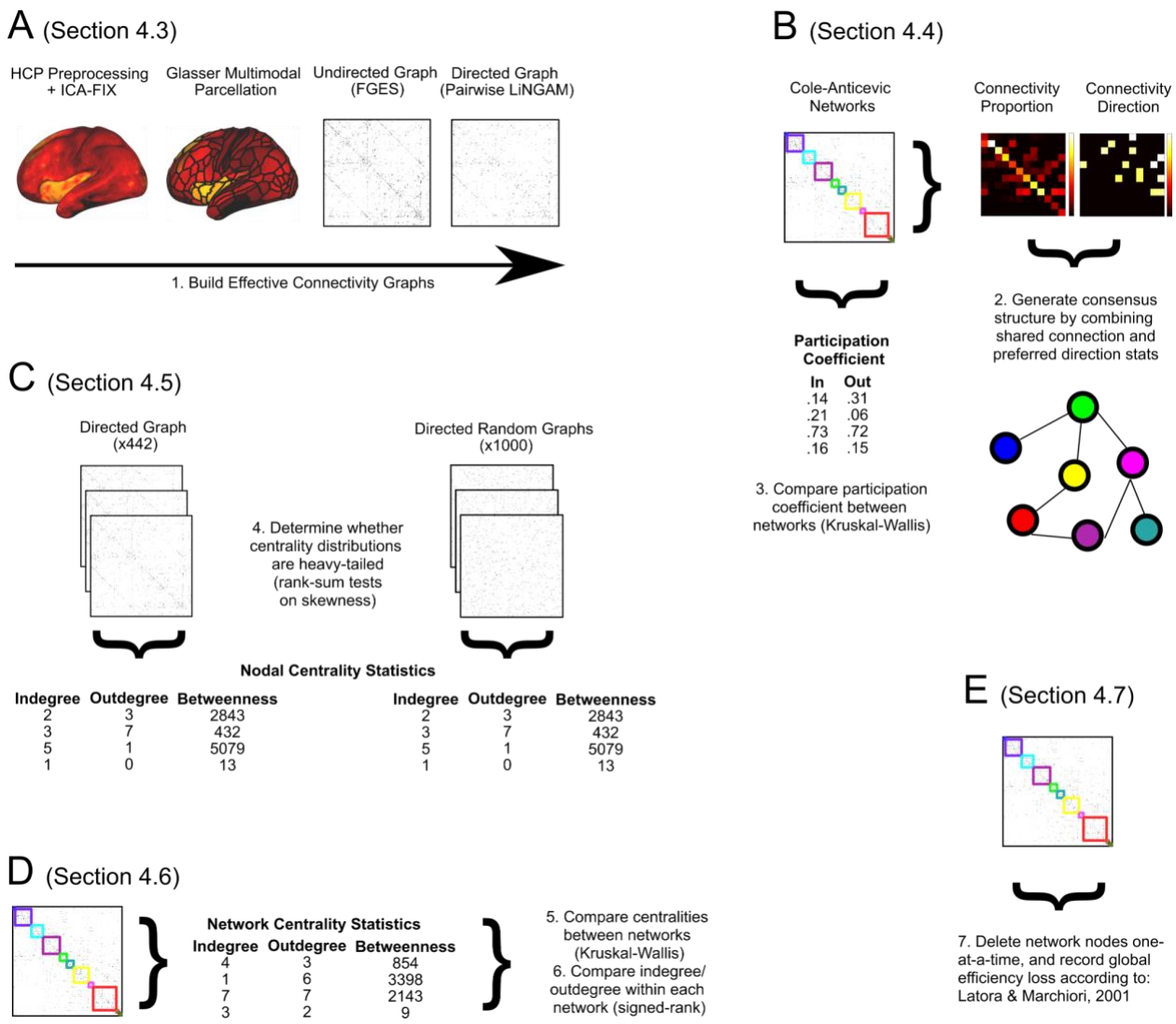

Figure 4. Summary of the strategy we employed to build single-subject (n = 442) effective connectivity graphs for further analysis, and the analyses we ran to characterize the hub structure of these RSNs.

***A**: Described in Section 4.3 (Methods) and Section 2.1 (Results).*

***B**: Described in Section 4.4 (Methods) and Section 2.2 (Results).*

***C**: Described in Section 4.5 (Methods) and Section 2.3 (Results).*

***D**: Described in Section 4.6 (Methods) and Section 2.4 (Results).*

***E**: Described in Section 4.7 (Methods) and Section 2.5 (Results).*

4.4 Resting-State Network Connectivity Statistics

For each subject and each of 12 resting-state RSNs (RSNs), we established whether the RSN shared a statistically significant proportion of connections with another RSN (*Figure 4b*) by calculating the total number of connections that the RSN shared with the other 11 RSNs (i.e. the sum total of out-of-RSN connections). Then, by dividing that sum total by 11, we arrive at a suitable null hypothesis of equal inter-RSN connectivity (i.e., that the RSN shared out-of-RSN connections equally between the other 11 RSNs). For each of the other 11 RSNs, we tested the actual number of shared between-RSN connections against the null hypothesis of equal connectivity to all 11 RSNs using Wilcoxon signed-rank tests, which we FDR-corrected (Benjamini & Hochberg, 1995) for multiple comparisons, thus establishing whether pairs of RSNs were significantly connected. To clarify the direction of causal connectivity between significantly connected pairs of RSNs, we calculated the proportion of causal connections from each RSN to each other RSN, then compared that proportion against a null hypothesis of 50% (i.e., that the connections between the pair of RSNs A & B are equally from A to B and from B to A) using Wilcoxon signed-rank tests (FDR-corrected for multiple comparisons). For each pair of RSNs found to be significant with reference to a null hypothesis of equal (i.e. random) inter-RSN connectivity, we calculated the effect size of the test for significant shared connections using Cohen's d, and masked inter-RSN connections that did not meet at least the threshold for a small effect size (Cohen's d >= 0.2). This analysis clarified a) which RSNs are significantly connected with at least a small effect size, and b) which RSNs significantly send (vs. receive) information to (vs. from) other RSNs. We supplemented this with an analysis of participation coefficient (a measure of the diversity of RSNs a node connects to), calculated separately for incoming and outgoing connections. We compared the average nodal participation coefficients in 12 established RSNs (Ji et al., 2019) that have been validated for our current parcellation using Kruskall-Wallis tests and conducted post-hoc tests using Tukey's honest significant difference (HSD).

4.5 Centrality Distributions in Human Cortex

For each effective connectivity graph, we calculated nodal (n = 360) centrality statistics using indegree (number of incoming connections), outdegree (number of outgoing connections), and betweenness centrality (number of shortest paths the node participates in) (*Figure 4b*). For an illustration of various centrality metrics including degree and betweenness, see Rubinov and Sporns (2010). To statistically quantify whether centrality-based cortical hubs existed on the basis of significantly heavy-tailed centrality distributions, we generated a reference set of 1000 random directed graphs with the same number of nodes (360) and connections as the cortical causal graphs (*Figure 4c*). We then used Wilcoxon rank-sum tests to compare the skewness of the effective connectivity graphs to the random directed graphs.

4.6 Resting-State Network Differences in Centrality-Based Hubs

We compared the average nodal centralities (degree, betweenness) in 12 established RSNs (Ji et al., 2019) that have been validated for our current parcellation (*Figure 4c*). For each subject, we calculated the average nodal indegree, outdegree, total degree, and betweenness centrality for nodes within each of these 12 RSNs. We compared centrality across the 12 RSNs using Kruskall-Wallis tests, and conducted post-hoc tests using Tukey's honest significant difference (HSD). Additionally, we compared indegree and outdegree within each of the 12 RSNs using Wilcoxon signed-rank tests, and FDR-corrected the resulting p-values for n = 12 multiple comparisons.

4.7 Network Vulnerability to Targeted Attack

To clarify the functional role of hubs in the effective cortical network, we subjected each subject's effective connectome to a targeted attack analysis. This method is useful for understanding brain network function, as lesions to hubs that connect many different brain subnetworks are particularly deleterious (Aerts et al., 2016), and gray matter abnormalities across many disorders are in hub nodes (Crossley et al., 2014). This method typically systematically deletes the most highly connected hub nodes and recording the connectome's global efficiency (the inverse shortest path lengths in the network, a

measure of overall efficiency of connectivity; Latora & Marchiori, 2001; Rubinov & Sporns, 2010) following node deletion.

To assess cortical vulnerability at the RSN level, we modified this method by instead deleting the nodes of each RSN (one at a time) from the individual subject-level cortical effective connectivity graphs, and we recorded changes in connectome communication efficiency as percent change in global efficiency (*Figure 4e*). We supplemented this targeted attack analysis with a random attack analysis, by deleting randomly selected nodes rather than specifically targeting nodes from one RSN at a time. To minimize order effects in the virtual lesion analysis we ran the analysis 10 times for every subject, deleting the nodes within each RSN in a random order each time, then we took the mean of the efficiency loss over the 10 runs. This resulted in a set of 13 loss-of-efficiency curves per subject that quantified how strongly communication was impaired as successive nodes from each RSN were deleted. We fit a linear regression to each subject's loss-of-efficiency lines (for each of 13 deletion schedules) and compared the slope of the linear regression fit between RSNs (plus random deletion) to quantify which RSN resulted in the most rapid loss-of-efficiency. RSN deletion slopes were statistically compared using a Kruskal-Wallis test with post-hoc significance testing using Tukey’s HSD. Additionally, we examined which nodes had the greatest overall impact on connectome loss-of-efficiency by deleting (in single subjects) each node (of 360) one at a time and recording the change in overall global efficiency.

References

Achard, S., & Bullmore, E. (2007). Efficiency and Cost of Economical Brain Functional Networks. *PLOS Computational Biology*, *3*(2), e17. https://doi.org/10.1371/journal.pcbi.0030017

Achard, S., Salvador, R., Whitcher, B., Suckling, J., & Bullmore, E. (2006). A Resilient, Low-Frequency, Small-World Human Brain Functional Network with Highly Connected Association Cortical Hubs. *Journal of Neuroscience*, *26*(1), 63–72. https://doi.org/10.1523/JNEUROSCI.3874-05.2006

Aerts, H., Fias, W., Caeyenberghs, K., & Marinazzo, D. (2016). Brain networks under attack: Robustness properties and the impact of lesions. *Brain*, *139*(12), 3063–3083. https://doi.org/10.1093/brain/aww194

Arnatkevičiūtė, A., Fulcher, B. D., Pocock, R., & Fornito, A. (2018). Hub connectivity, neuronal diversity, and gene expression in the Caenorhabditis elegans connectome. *PLOS Computational Biology*, *14*(2), e1005989. https://doi.org/10.1371/journal.pcbi.1005989

Assem, M., Glasser, M. F., Van Essen, D. C., & Duncan, J. (2020). A Domain-General Cognitive Core Defined in Multimodally Parcellated Human Cortex. *Cerebral Cortex*, *30*(8), 4361–4380. https://doi.org/10.1093/cercor/bhaa023

Badre, D., & Nee, D. E. (2018). Frontal cortex and the hierarchical control of behavior. *Trends in Cognitive Sciences*, *22*(2), 170–188. https://doi.org/10.1016/j.tics.2017.11.005

Barch, D. M., Burgess, G. C., Harms, M. P., Petersen, S. E., Schlaggar, B. L., Corbetta, M., Glasser, M. F., Curtiss, S., Dixit, S., Feldt, C., Nolan, D., Bryant, E., Hartley, T., Footer, O., Bjork, J. M., Poldrack, R., Smith, S., Johansen-Berg, H., Snyder, A. Z., & Van Essen, D. C. (2013). Function in the human connectome: Task-fMRI and individual differences in behavior. *NeuroImage*, *80*, 169–189. https://doi.org/10.1016/j.neuroimage.2013.05.033

Belsher, B. E., Beech, E. H., Reddy, M. K., Smolenski, D. J., Rauch, S. A. M., Kelber, M., Issa, F., Lewis, C., & Bisson, J. I. (2021). Advances in repetitive transcranial magnetic stimulation for

posttraumatic stress disorder: A systematic review. *Journal of Psychiatric Research*, *138*, 598–606. https://doi.org/10.1016/j.jpsychires.2021.05.011

Benjamini, Y., & Hochberg, Y. (1995). Controlling the False Discovery Rate: A Practical and Powerful Approach to Multiple Testing. *Journal of the Royal Statistical Society. Series B (Methodological)*, *57*(1), 289–300. JSTOR.

Bertolero, M. A., Yeo, B. T. T., Bassett, D. S., & D'Esposito, M. (2018). A mechanistic model of connector hubs, modularity and cognition. *Nature Human Behaviour*, *2*(10), 765–777. https://doi.org/10.1038/s41562-018-0420-6

Bressler, S. L. (1995). Large-scale cortical networks and cognition. *Brain Research Reviews*, *20*(3), 288–304. https://doi.org/10.1016/0165-0173(94)00016-I

Buckner, R. L., Sepulcre, J., Talukdar, T., Krienen, F. M., Liu, H., Hedden, T., Andrews-Hanna, J. R., Sperling, R. A., & Johnson, K. A. (2009). Cortical Hubs Revealed by Intrinsic Functional Connectivity: Mapping, Assessment of Stability, and Relation to Alzheimer's Disease. *Journal of Neuroscience*, *29*(6), 1860–1873. https://doi.org/10.1523/JNEUROSCI.5062-08.2009

Bullmore, E., & Sporns, O. (2009). Complex brain networks: Graph theoretical analysis of structural and functional systems. *Nature Reviews. Neuroscience*, *10*(3), 186–198. https://doi.org/10.1038/nrn2575

Bullmore, E. T., & Bassett, D. S. (2011). Brain graphs: Graphical models of the human brain connectome. *Annual Review of Clinical Psychology*, *7*, 113–140. https://doi.org/10.1146/annurev-clinpsy-040510-143934

Chickering, D. M. (2002). *Optimal Structure Identification With Greedy Search*. 48.

Cocuzza, C. V., Ito, T., Schultz, D., Bassett, D. S., & Cole, M. W. (2020). Flexible Coordinator and Switcher Hubs for Adaptive Task Control. *Journal of Neuroscience*, *40*(36), 6949–6968. https://doi.org/10.1523/JNEUROSCI.2559-19.2020

Cole, M. W., Pathak, S., & Schneider, W. (2010). Identifying the brain's most globally connected regions. *NeuroImage*, *49*(4), 3132–3148. https://doi.org/10.1016/j.neuroimage.2009.11.001

Cole, M. W., Reynolds, J. R., Power, J. D., Repovs, G., Anticevic, A., & Braver, T. S. (2013). Multi-task connectivity reveals flexible hubs for adaptive task control. *Nature Neuroscience*, *16*(9), 1348–1355. https://doi.org/10.1038/nn.3470

Corbetta, M., & Shulman, G. L. (2002). Control of goal-directed and stimulus-driven attention in the brain. *Nature Reviews Neuroscience*, *3*(3), 201–215. https://doi.org/10.1038/nrn755

Cornblath, E. J., Tang, E., Baum, G. L., Moore, T. M., Adebimpe, A., Roalf, D. R., Gur, R. C., Gur, R. E., Pasqualetti, F., Satterthwaite, T. D., & Bassett, D. S. (2019). Sex differences in network controllability as a predictor of executive function in youth. *NeuroImage*, *188*, 122–134. https://doi.org/10.1016/j.neuroimage.2018.11.048

Crittenden, B. M., Mitchell, D. J., & Duncan, J. (2016). Task Encoding across the Multiple Demand Cortex Is Consistent with a Frontoparietal and Cingulo-Opercular Dual Networks Distinction. *The Journal of Neuroscience*, *36*(23), 6147–6155. https://doi.org/10.1523/JNEUROSCI.4590-15.2016

Crossley, N. A., Mechelli, A., Scott, J., Carletti, F., Fox, P. T., McGuire, P., & Bullmore, E. T. (2014). The hubs of the human connectome are generally implicated in the anatomy of brain disorders. *Brain: A Journal of Neurology*, *137*(Pt 8), 2382–2395. https://doi.org/10.1093/brain/awu132

Crossley, N. A., Mechelli, A., Vertes, P. E., Winton-Brown, T. T., Patel, A. X., Ginestet, C. E., McGuire, P., & Bullmore, E. T. (2013). Cognitive relevance of the community structure of the human brain functional coactivation network. *Proceedings of the National Academy of Sciences*, *110*(28), 11583–11588. https://doi.org/10.1073/pnas.1220826110

Del Fabro, L., Schmidt, A., Fortea, L., Delvecchio, G., D'Agostino, A., Radua, J., Borgwardt, S., & Brambilla, P. (2021). Functional brain network dysfunctions in subjects at high-risk for psychosis: A meta-analysis of resting-state functional connectivity. *Neuroscience & Biobehavioral Reviews*, *128*, 90–101. https://doi.org/10.1016/j.neubiorev.2021.06.020

Dosenbach, N. U. F., Fair, D. A., Cohen, A. L., Schlaggar, B. L., & Petersen, S. E. (2008). A dual-networks architecture of top-down control. *Trends in Cognitive Sciences*, *12*(3), 99–105. https://doi.org/10.1016/j.tics.2008.01.001

Dosenbach, N. U. F., Visscher, K. M., Palmer, E. D., Miezin, F. M., Wenger, K. K., Kang, H. C., Burgund, E. D., Grimes, A. L., Schlaggar, B. L., & Petersen, S. E. (2006). A core system for the implementation of task sets. *Neuron*, *50*(5), 799–812. https://doi.org/10.1016/j.neuron.2006.04.031

Duncan, J. (2010). The multiple-demand (MD) system of the primate brain: Mental programs for intelligent behaviour. *Trends in Cognitive Sciences*, *14*(4), 172–179. https://doi.org/10.1016/j.tics.2010.01.004

Eguiluz, V. M., Chialvo, D. R., Cecchi, G. A., Baliki, M., & Apkarian, A. V. (2005). Scale-free brain functional networks. *Physical Review Letters*, *94*(1), 018102. https://doi.org/10.1103/PhysRevLett.94.018102

Fair, D. A., Dosenbach, N. U. F., Church, J. A., Cohen, A. L., Brahmbhatt, S., Miezin, F. M., Barch, D. M., Raichle, M. E., Petersen, S. E., & Schlaggar, B. L. (2007). Development of distinct control networks through segregation and integration. *Proceedings of the National Academy of Sciences*, *104*(33), 13507–13512. https://doi.org/10.1073/pnas.0705843104

Ferrarelli, F., & Phillips, M. L. (2021). PFC neuromodulation with theta burst stimulation to impact behavior and neural network activity in schizophrenia and bipolar disorder. *Neuropsychopharmacology*, 1–2. https://doi.org/10.1038/s41386-021-01086-3

Fitzgerald, P. B. (2021). Targeting repetitive transcranial magnetic stimulation in depression: Do we really know what we are stimulating and how best to do it? *Brain Stimulation*, *14*(3), 730–736. https://doi.org/10.1016/j.brs.2021.04.018

Frässle, S., Harrison, S. J., Heinzle, J., Clementz, B. A., Tamminga, C. A., Sweeney, J. A., Gershon, E. S., Keshavan, M. S., Pearlson, G. D., Powers, A., & Stephan, K. E. (2021). Regression dynamic

causal modeling for resting-state fMRI. *Human Brain Mapping*, *42*(7), 2159–2180. https://doi.org/10.1002/hbm.25357

Friston, K. (2002). Beyond Phrenology: What Can Neuroimaging Tell Us About Distributed Circuitry? *Annual Review of Neuroscience*, *25*(1), 221–250. https://doi.org/10.1146/annurev.neuro.25.112701.142846

Friston, K. J., Harrison, L., & Penny, W. (2003). Dynamic causal modelling. *NeuroImage*, *19*(4), 1273–1302. https://doi.org/10.1016/S1053-8119(03)00202-7

Gates, K. M., & Molenaar, P. C. M. (2012). Group search algorithm recovers effective connectivity maps for individuals in homogeneous and heterogeneous samples. *NeuroImage*, *63*(1), 310–319. https://doi.org/10.1016/j.neuroimage.2012.06.026

Glasser, M. F., Coalson, T. S., Robinson, E. C., Hacker, C. D., Harwell, J., Yacoub, E., Ugurbil, K., Andersson, J., Beckmann, C. F., Jenkinson, M., Smith, S. M., & Van Essen, D. C. (2016). A multi-modal parcellation of human cerebral cortex. *Nature*, *536*(7615), 171–178. https://doi.org/10.1038/nature18933

Glasser, M. F., Sotiropoulos, S. N., Wilson, J. A., Coalson, T. S., Fischl, B., Andersson, J. L., Xu, J., Jbabdi, S., Webster, M., Polimeni, J. R., Van Essen, D. C., & Jenkinson, M. (2013). The minimal preprocessing pipelines for the Human Connectome Project. *NeuroImage*, *80*, 105–124. https://doi.org/10.1016/j.neuroimage.2013.04.127

Granger, C. W. J. (1969). Investigating Causal Relations by Econometric Models and Cross-spectral Methods. *Econometrica*, *37*(3), 424–438. https://doi.org/10.2307/1912791

Gratton, C., Sun, H., & Petersen, S. E. (2018). Control networks and hubs. *Psychophysiology*, *55*(3), e13032. https://doi.org/10.1111/psyp.13032

Grayson, D. S., Ray, S., Carpenter, S., Iyer, S., Dias, T. G. C., Stevens, C., Nigg, J. T., & Fair, D. A. (2014). Structural and Functional Rich Club Organization of the Brain in Children and Adults. *PLOS ONE*, *9*(2), e88297. https://doi.org/10.1371/journal.pone.0088297

Griffanti, L., Salimi-Khorshidi, G., Beckmann, C. F., Auerbach, E. J., Douaud, G., Sexton, C. E., Zsoldos, E., Ebmeier, K. P., Filippini, N., Mackay, C. E., Moeller, S., Xu, J., Yacoub, E., Baselli, G., Ugurbil, K., Miller, K. L., & Smith, S. M. (2014). ICA-based artefact removal and accelerated fMRI acquisition for improved resting state network imaging. *NeuroImage*, *95*, 232–247. https://doi.org/10.1016/j.neuroimage.2014.03.034

Gu, S., Pasqualetti, F., Cieslak, M., Telesford, Q. K., Yu, A. B., Kahn, A. E., Medaglia, J. D., Vettel, J. M., Miller, M. B., Grafton, S. T., & Bassett, D. S. (2015). Controllability of structural brain networks. *Nature Communications*, *6*(1), 8414. https://doi.org/10.1038/ncomms9414

Hearne, L., Cocchi, L., Zalesky, A., & Mattingley, J. B. (2015). Interactions between default mode and control networks as a function of increasing cognitive reasoning complexity. *Human Brain Mapping*, *36*(7), 2719–2731. https://doi.org/10.1002/hbm.22802

Hellyer, P. J., Shanahan, M., Scott, G., Wise, R. J. S., Sharp, D. J., & Leech, R. (2014). The Control of Global Brain Dynamics: Opposing Actions of Frontoparietal Control and Default Mode Networks on Attention. *Journal of Neuroscience*, *34*(2), 451–461. https://doi.org/10.1523/JNEUROSCI.1853-13.2014

Huckins, J. F., Adeyemo, B., Miezin, F. M., Power, J. D., Gordon, E. M., Laumann, T. O., Heatherton, T. F., Petersen, S. E., & Kelley, W. M. (2019). Reward-related regions form a preferentially coupled system at rest. *Human Brain Mapping*, *40*(2), 361–376. https://doi.org/10.1002/hbm.24377

Hyvärinen, A., & Smith, S. M. (2013). Pairwise Likelihood Ratios for Estimation of Non-Gaussian Structural Equation Models. *Journal of Machine Learning Research: JMLR*, *14*(Jan), 111–152.

Jalili, M., Salehzadeh-Yazdi, A., Asgari, Y., Arab, S. S., Yaghmaie, M., Ghavamzadeh, A., & Alimoghaddam, K. (2015). CentiServer: A Comprehensive Resource, Web-Based Application and R Package for Centrality Analysis. *PLOS ONE*, *10*(11), e0143111. https://doi.org/10.1371/journal.pone.0143111

Ji, J. L., Spronk, M., Kulkarni, K., Repovš, G., Anticevic, A., & Cole, M. W. (2019). Mapping the human brain's cortical-subcortical functional network organization. *NeuroImage*, *185*, 35–57. https://doi.org/10.1016/j.neuroimage.2018.10.006

Kelly, A. M. C., Uddin, L. Q., Biswal, B. B., Castellanos, F. X., & Milham, M. P. (2008). Competition between functional brain networks mediates behavioral variability. *NeuroImage*, *39*(1), 527–537. https://doi.org/10.1016/j.neuroimage.2007.08.008

Latora, V., & Marchiori, M. (2001). Efficient behavior of small-world networks. *Physical Review Letters*, *87*(19), 198701. https://doi.org/10.1103/PhysRevLett.87.198701

Lee, W. H., Rodrigue, A., Glahn, D. C., Bassett, D. S., & Frangou, S. (2020). Heritability and Cognitive Relevance of Structural Brain Controllability. *Cerebral Cortex*, *30*(5), 3044–3054. https://doi.org/10.1093/cercor/bhz293

Long, N. M., & Kuhl, B. A. (2018). Bottom-Up and Top-Down Factors Differentially Influence Stimulus Representations Across Large-Scale Attentional Networks. *Journal of Neuroscience*, *38*(10), 2495–2504. https://doi.org/10.1523/JNEUROSCI.2724-17.2018

Marcus, D. S., Harms, M. P., Snyder, A. Z., Jenkinson, M., Wilson, J. A., Glasser, M. F., Barch, D. M., Archie, K. A., Burgess, G. C., Ramaratnam, M., Hodge, M., Horton, W., Herrick, R., Olsen, T., McKay, M., House, M., Hileman, M., Reid, E., Harwell, J., … Van Essen, D. C. (2013). Human Connectome Project informatics: Quality control, database services, and data visualization. *NeuroImage*, *80*, 202–219. https://doi.org/10.1016/j.neuroimage.2013.05.077

Marek, S., & Dosenbach, N. U. F. (2018). The frontoparietal network: Function, electrophysiology, and importance of individual precision mapping. *Dialogues in Clinical Neuroscience*, *20*(2), 133–140.

Marek, S., Hwang, K., Foran, W., Hallquist, M. N., & Luna, B. (2015). The Contribution of Network Organization and Integration to the Development of Cognitive Control. *PLOS Biology*, *13*(12), e1002328. https://doi.org/10.1371/journal.pbio.1002328

McIntosh, A. R. (2000). Towards a network theory of cognition. *Neural Networks*, *13*(8), 861–870. https://doi.org/10.1016/S0893-6080(00)00059-9

Meunier, D., Lambiotte, R., & Bullmore, E. T. (2010). Modular and hierarchically modular organization of brain networks. *Frontiers in Neuroscience*, *4*, 200. https://doi.org/10.3389/fnins.2010.00200

Meunier, D., Lambiotte, R., Fornito, A., Ersche, K. D., & Bullmore, E. T. (2009). Hierarchical modularity in human brain functional networks. *Frontiers in Neuroinformatics*, *3*, 37. https://doi.org/10.3389/neuro.11.037.2009

Mizzi, S., Pedersen, M., Lorenzetti, V., Heinrichs, M., & Labuschagne, I. (2021). Resting-state neuroimaging in social anxiety disorder: A systematic review. *Molecular Psychiatry*, 1–16. https://doi.org/10.1038/s41380-021-01154-6

Müller, R.-A., & Fishman, I. (2018). Brain Connectivity and Neuroimaging of Social Networks in Autism. *Trends in Cognitive Sciences*, *22*(12), 1103–1116. https://doi.org/10.1016/j.tics.2018.09.008

Mumford, J. A., & Ramsey, J. D. (2014). Bayesian networks for fMRI: A primer. *NeuroImage*, *86*, 573–582. https://doi.org/10.1016/j.neuroimage.2013.10.020

Murphy, A. C., Bertolero, M. A., Papadopoulos, L., Lydon-Staley, D. M., & Bassett, D. S. (2020). Multimodal network dynamics underpinning working memory. *Nature Communications*, *11*(1), 3035. https://doi.org/10.1038/s41467-020-15541-0

Newbold, D. J., Gordon, E. M., Laumann, T. O., Seider, N. A., Montez, D. F., Gross, S. J., Zheng, A., Nielsen, A. N., Hoyt, C. R., Hampton, J. M., Ortega, M., Adeyemo, B., Miller, D. B., Van, A. N., Marek, S., Schlaggar, B. L., Carter, A. R., Kay, B. P., Greene, D. J., … Dosenbach, N. U. F. (2021). Cingulo-opercular control network and disused motor circuits joined in standby mode. *Proceedings of the National Academy of Sciences*, *118*(13). https://doi.org/10.1073/pnas.2019128118

Oldham, S., & Fornito, A. (2019). The development of brain network hubs. *Developmental Cognitive Neuroscience*, *36*, 100607. https://doi.org/10.1016/j.dcn.2018.12.005

Oldham, S., Fulcher, B., Parkes, L., Arnatkevičiūtė, A., Suo, C., & Fornito, A. (2019). Consistency and differences between centrality measures across distinct classes of networks. *PLOS ONE*, *14*(7), e0220061. https://doi.org/10.1371/journal.pone.0220061

Pavlovic, D. M., Vértes, P. E., Bullmore, E. T., Schafer, W. R., & Nichols, T. E. (2014). Stochastic Blockmodeling of the Modules and Core of the Caenorhabditis elegans Connectome. *PLOS ONE*, *9*(7), e97584. https://doi.org/10.1371/journal.pone.0097584

Power, J. D., Schlaggar, B. L., Lessov-Schlaggar, C. N., & Petersen, S. E. (2013). Evidence for hubs in human functional brain networks. *Neuron*, *79*(4). https://doi.org/10.1016/j.neuron.2013.07.035

Ramsey, J. D. (2015). *Scaling Up Greedy Causal Search for Continuous Variables*.

Ramsey, J. D., Hanson, S. J., Hanson, C., Halchenko, Y. O., Poldrack, R. A., & Glymour, C. (2010). Six problems for causal inference from fMRI. *NeuroImage*, *49*(2), 1545–1558. https://doi.org/10.1016/j.neuroimage.2009.08.065

Ramsey, J. D., Sanchez-Romero, R., & Glymour, C. (2014). Non-Gaussian methods and high-pass filters in the estimation of effective connections. *NeuroImage*, *84*, 986–1006. https://doi.org/10.1016/j.neuroimage.2013.09.062

Ramsey, J., Glymour, M., Sanchez-Romero, R., & Glymour, C. (2017). A million variables and more: The Fast Greedy Equivalence Search algorithm for learning high-dimensional graphical causal models, with an application to functional magnetic resonance images. *International Journal of Data Science and Analytics*, *3*(2), 121–129. https://doi.org/10.1007/s41060-016-0032-z

Rawls, E., Kummerfeld, E., & Zilverstand, A. (2021). An integrated multimodal model of alcohol use disorder generated by data-driven causal discovery analysis. *Communications Biology*, *4*(1), 1–12. https://doi.org/10.1038/s42003-021-01955-z

Ray, K. L., Ragland, J. D., MacDonald, A. W., Gold, J. M., Silverstein, S. M., Barch, D. M., & Carter, C. S. (2020). Dynamic reorganization of the frontal parietal network during cognitive control and episodic memory. *Cognitive, Affective, & Behavioral Neuroscience*, *20*(1), 76–90. https://doi.org/10.3758/s13415-019-00753-9

Reber, J., Hwang, K., Bowren, M., Bruss, J., Mukherjee, P., Tranel, D., & Boes, A. D. (2021). Cognitive impairment after focal brain lesions is better predicted by damage to structural than functional network hubs. *Proceedings of the National Academy of Sciences*, *118*(19). https://doi.org/10.1073/pnas.2018784118

Reid, A. T., Headley, D. B., Mill, R. D., Sanchez-Romero, R., Uddin, L. Q., Marinazzo, D., Lurie, D. J., Valdés-Sosa, P. A., Hanson, S. J., Biswal, B. B., Calhoun, V., Poldrack, R. A., & Cole, M. W. (2019). Advancing functional connectivity research from association to causation. *Nature Neuroscience*, *22*(11), 1751–1760. https://doi.org/10.1038/s41593-019-0510-4

Robinson, E. C., Jbabdi, S., Glasser, M. F., Andersson, J., Burgess, G. C., Harms, M. P., Smith, S. M., Van Essen, D. C., & Jenkinson, M. (2014). MSM: A new flexible framework for Multimodal Surface Matching. *NeuroImage*, *100*, 414–426. https://doi.org/10.1016/j.neuroimage.2014.05.069

Rubinov, M., & Sporns, O. (2010). Complex network measures of brain connectivity: Uses and interpretations. *NeuroImage*, *52*(3), 1059–1069. https://doi.org/10.1016/j.neuroimage.2009.10.003

Rubinov, M., Ypma, R. J. F., Watson, C., & Bullmore, E. T. (2015). Wiring cost and topological participation of the mouse brain connectome. *Proceedings of the National Academy of Sciences of the United States of America*, *112*(32), 10032–10037. https://doi.org/10.1073/pnas.1420315112

Salimi-Khorshidi, G., Douaud, G., Beckmann, C. F., Glasser, M. F., Griffanti, L., & Smith, S. M. (2014). Automatic denoising of functional MRI data: Combining independent component analysis and hierarchical fusion of classifiers. *NeuroImage*, *90*, 449–468. https://doi.org/10.1016/j.neuroimage.2013.11.046

Sanchez-Romero, R., Ramsey, J. D., Zhang, K., Glymour, M. R. K., Huang, B., & Glymour, C. (2019). Estimating feedforward and feedback effective connections from fMRI time series: Assessments of statistical methods. *Network Neuroscience*, *3*(2), 274–306. https://doi.org/10.1162/netn_a_00061

Schwarz, G. (1978). *Estimating the Dimension of a Model*.

Smith, S. M. (2012). The future of FMRI connectivity. *NeuroImage*, *62*(2), 1257–1266. https://doi.org/10.1016/j.neuroimage.2012.01.022

Smith, S. M., Beckmann, C. F., Andersson, J., Auerbach, E. J., Bijsterbosch, J., Douaud, G., Duff, E., Feinberg, D. A., Griffanti, L., Harms, M. P., Kelly, M., Laumann, T., Miller, K. L., Moeller, S., Petersen, S., Power, J., Salimi-Khorshidi, G., Snyder, A. Z., Vu, A. T., … Glasser, M. F. (2013). Resting-state fMRI in the Human Connectome Project. *NeuroImage*, *80*, 144–168. https://doi.org/10.1016/j.neuroimage.2013.05.039

Smith, S. M., Miller, K. L., Salimi-Khorshidi, G., Webster, M., Beckmann, C. F., Nichols, T. E., Ramsey, J. D., & Woolrich, M. W. (2011). Network modelling methods for FMRI. *NeuroImage*, *54*(2), 875–891. https://doi.org/10.1016/j.neuroimage.2010.08.063

Smith, S. M., Nichols, T. E., Vidaurre, D., Winkler, A. M., Behrens, T. E. J., Glasser, M. F., Ugurbil, K., Barch, D. M., Van Essen, D. C., & Miller, K. L. (2015). A positive-negative mode of population covariation links brain connectivity, demographics and behavior. *Nature Neuroscience*, *18*(11), 1565–1567. https://doi.org/10.1038/nn.4125

Sohn, Y., Choi, M.-K., Ahn, Y.-Y., Lee, J., & Jeong, J. (2011). Topological Cluster Analysis Reveals the Systemic Organization of the Caenorhabditis elegans Connectome. *PLOS Computational Biology*, *7*(5), e1001139. https://doi.org/10.1371/journal.pcbi.1001139

Song, S., Zilverstand, A., Gui, W., Li, H., & Zhou, X. (2019). Effects of single-session versus multi-session non-invasive brain stimulation on craving and consumption in individuals with drug addiction, eating disorders or obesity: A meta-analysis. *Brain Stimulation*, *12*(3), 606–618. https://doi.org/10.1016/j.brs.2018.12.975

Sporns, O. (2012). *Discovering the Human Connectome*. MIT Press.

Sporns, O. (2013). The human connectome: Origins and challenges. *NeuroImage*, *80*, 53–61. https://doi.org/10.1016/j.neuroimage.2013.03.023

Sporns, O., Honey, C. J., & Kötter, R. (2007). Identification and Classification of Hubs in Brain Networks. *PLOS ONE*, *2*(10), e1049. https://doi.org/10.1371/journal.pone.0001049

Sporns, O., Tononi, G., & Kötter, R. (2005). The Human Connectome: A Structural Description of the Human Brain. *PLOS Computational Biology*, *1*(4), e42. https://doi.org/10.1371/journal.pcbi.0010042

Tang, E., Giusti, C., Baum, G. L., Gu, S., Pollock, E., Kahn, A. E., Roalf, D. R., Moore, T. M., Ruparel, K., Gur, R. C., Gur, R. E., Satterthwaite, T. D., & Bassett, D. S. (2017). Developmental increases in white matter network controllability support a growing diversity of brain dynamics. *Nature Communications*, *8*(1), 1252. https://doi.org/10.1038/s41467-017-01254-4

Taylor, J. J., Kurt, H. G., & Anand, A. (2021). Resting State Functional Connectivity Biomarkers of Treatment Response in Mood Disorders: A Review. *Frontiers in Psychiatry*, *0*. https://doi.org/10.3389/fpsyt.2021.565136

Tomasi, D., & Volkow, N. D. (2011). Functional connectivity hubs in the human brain. *NeuroImage*, *57*(3), 908–917. https://doi.org/10.1016/j.neuroimage.2011.05.024

Uğurbil, K., Xu, J., Auerbach, E. J., Moeller, S., Vu, A. T., Duarte-Carvajalino, J. M., Lenglet, C., Wu, X., Schmitter, S., Van de Moortele, P. F., Strupp, J., Sapiro, G., De Martino, F., Wang, D., Harel, N., Garwood, M., Chen, L., Feinberg, D. A., Smith, S. M., … Yacoub, E. (2013). Pushing spatial and temporal resolution for functional and diffusion MRI in the Human Connectome Project. *NeuroImage*, *80*, 80–104. https://doi.org/10.1016/j.neuroimage.2013.05.012

Valdes-Sosa, P. A., Roebroeck, A., Daunizeau, J., & Friston, K. (2011). Effective connectivity: Influence, causality and biophysical modeling. *NeuroImage*, *58*(2), 339–361. https://doi.org/10.1016/j.neuroimage.2011.03.058

van den Heuvel, M. P., & Sporns, O. (2013). Network hubs in the human brain. *Trends in Cognitive Sciences*, *17*(12), 683–696. https://doi.org/10.1016/j.tics.2013.09.012

Van Essen, D. C., Smith, S. M., Barch, D. M., Behrens, T. E. J., Yacoub, E., & Ugurbil, K. (2013). The WU-Minn Human Connectome Project: An overview. *NeuroImage*, *80*, 62–79. https://doi.org/10.1016/j.neuroimage.2013.05.041

Van Essen, D. C., & Ugurbil, K. (2012). The future of the human connectome. *NeuroImage*, *62*(2), 1299–1310. https://doi.org/10.1016/j.neuroimage.2012.01.032

Varshney, L. R., Chen, B. L., Paniagua, E., Hall, D. H., & Chklovskii, D. B. (2011). Structural Properties of the Caenorhabditis elegans Neuronal Network. *PLOS Computational Biology*, *7*(2), e1001066. https://doi.org/10.1371/journal.pcbi.1001066

Voigt, J. D., Leuchter, A. F., & Carpenter, L. L. (2021). Theta burst stimulation for the acute treatment of major depressive disorder: A systematic review and meta-analysis. *Translational Psychiatry*, *11*(1), 330. https://doi.org/10.1038/s41398-021-01441-4

Vossel, S., Geng, J. J., & Fink, G. R. (2014). Dorsal and Ventral Attention Systems: Distinct Neural Circuits but Collaborative Roles. *The Neuroscientist*, *20*(2), 150–159. https://doi.org/10.1177/1073858413494269

White, J. G., Southgate, E., Thomson, J. N., & Brenner, S. (1986). The structure of the nervous system of the nematode Caenorhabditis elegans. *Philosophical Transactions of the Royal Society of London. B, Biological Sciences*, *314*(1165), 1–340. https://doi.org/10.1098/rstb.1986.0056

Zhang, R., Lam, C. L. M., Peng, X., Zhang, D., Zhang, C., Huang, R., & Lee, T. M. C. (2021). Efficacy and acceptability of transcranial direct current stimulation for treating depression: A meta-analysis of randomized controlled trials. *Neuroscience & Biobehavioral Reviews*, *126*, 481–490. https://doi.org/10.1016/j.neubiorev.2021.03.026

Zilverstand, A., O'Halloran, R., & Goldstein, R. Z. (2018). Resting-State and Structural Brain Connectivity in Individuals with Stimulant Addiction: A systematic review. In *The Routledge Handbook of Philosophy and Science of Addiction*. Routledge.

Zilverstand, A., Parvaz, M. A., & Goldstein, R. Z. (2017). Neuroimaging cognitive reappraisal in clinical populations to define neural targets for enhancing emotion regulation. A systematic review. *NeuroImage*, *151*, 105–116. https://doi.org/10.1016/j.neuroimage.2016.06.009

Zilverstand, A., Parvaz, M. A., Moeller, S. J., & Goldstein, R. Z. (2016). Cognitive interventions for addiction medicine: Understanding the underlying neurobiological mechanisms. *Progress in Brain Research*, *224*, 285–304. https://doi.org/10.1016/bs.pbr.2015.07.019

Zuo, X.-N., Ehmke, R., Mennes, M., Imperati, D., Castellanos, F. X., Sporns, O., & Milham, M. P. (2012). Network Centrality in the Human Functional Connectome. *Cerebral Cortex*, *22*(8), 1862–1875. https://doi.org/10.1093/cercor/bhr269